Pramāṇa, Vol. 22, Nos 3 & 4, March & April 1984, pp. 203–212. © Printed in India.

# Some features of the perturbing effects of gravity near the gas liquid critical point

S CHATTERJEE, V VANI and E S R GOPAL
Department of Physics, Indian Institute of Science, Bangalore 560012, India

**Abstract.** The effect of gravity on various thermodynamic properties near the gas-liquid critical point has been calculated. Using a simple equation satisfying scaling requirements, an analytic expression for density profile is obtained, using which the effect on different thermodynamic properties can be easily calculated.

**Keywords.** Critical point; gravity effect.

## 1. Introduction

Various physical systems near their critical points exhibit singular behaviour in many of the thermodynamic properties (Stanley 1971). Their singularities can be expressed in terms of the critical exponents which have nearly identical values for systems belonging to the same universality class. For a one-component fluid system the critical point is defined by assigning the value of the critical density and the critical temperature. In our following discussion the effect of gravity on some of the experimentally observed properties near the critical point of a fluid system is discussed. The experimental sample being confined within a cell of finite height, a density gradient develops in the fluid because of gravity. Near the critical point, the compressibility of the fluid being divergent, the hydrostatic pressure of the fluid column alters the density significantly along the height of the cell. The rest of the cell being away from the critical density, the critical divergences are smeared out in the observed data (Sengers and Sengers 1978; Moldover *et al* 1979; Kumar *et al* 1983).

The previous work of Hohenberg and Barmatz (1972) tackles the above problem with extensive numerical calculations. The starting point of their work assumes a parametric equation within the linear regime,

$$(\rho - \rho_c)/\rho_c = K(\theta) r^{\beta},$$

where $\rho$ is the density of the fluid and $\rho_c$ is the critical density. The parameters $\theta$, $r$ and $\beta$ are defined in their paper.

In our case we have assumed a simpler equation, to satisfy the scaling requirements, in the leading order in $\Delta\rho$ and $\Delta T$. This particular choice simplifies the calculation of the density profile and enables us to present analytic expressions for the variation of $\rho(z)$ with $z$. The convenience with this simple choice is that the distribution of density can be expressed in terms of a simple algebraic equation, which facilitates in arriving at numerical estimates of various quantities of interest. With this functional dependence we have calculated the effect of gravity on the isothermal compressibility, thermal expansion and velocity of sound. The typical values of parameters are chosen for the system Xe, which has been extensively studied. A preliminary version of the work is being published (Chatterjee *et al* 1983).

Section 2 of this paper deals with the theoretical calculations on the effect of gravity on various quantities of interest. Section 3 presents the results of the computations and compares the numerical values of our computations with other results in the literature.

## 2. Theory

### 2.1 *Determination of the density profile*

The density profile $\rho(z)$ of the fluid is derived by solving the well known hydrostatic stability relation

$$dP/dz = \rho g,$$

where the height $z$ is measured from the top of the cell and $g$ represents the acceleration due to gravity, $P$ being the pressure at any point in the cell.

Using $K_T = (1/\rho)(\partial\rho/\partial P)_T$ as the isothermal compressibility the above equation yields

$$d\rho/dz = g\rho^2 K_T. \tag{1}$$

It is obvious from (2) that due to large $K_T$, at the critical point, substantial density gradient appears for any finite value of $g$.

From the scaling theory, it is known

$$K_T^{-1} \sim |\Delta\rho^*|^{(\delta-1)}[1 + a_1\tilde{X} + a_2\tilde{X}^2 + \ldots]$$

for $\tilde{X} \ll 1$

with $\tilde{X} = t/|\Delta\rho^*|^{\mu/\nu d}$

and $K_T^{-1} \sim t^\gamma[1 + b_1\tilde{Y} + b_2\tilde{Y}^2 + \ldots]$ for $\tilde{Y} \ll 1$

with $\tilde{Y} = |\Delta\rho^*|^{2/\delta}/t^{2\nu/\mu}$

where $t = |(T - T_c)/T_c|$ and $|\Delta\rho^*| \equiv |(\rho - \rho_c)/\rho_c|$

and the indices, $\mu$, $\nu$, $d$, ... satisfy the equalities,

$$(\mu_{\delta-1})\delta = 1 \quad \text{and} \quad \nu(d - 2/\mu) = \nu$$

$d$ being the dimensionality of the system, $-3$ in our present case.

Retaining only upto the leading orders in $t$ and $|\Delta\rho^*|$ we get

$$K_T \sim K_T^0/[t^\gamma + a_1|\Delta\rho^*|^{\delta-1}]. \tag{2}$$

From (1) and (2) we have

$$d\rho/dz = \frac{g\rho^2(z)K_T^0}{[t^\gamma + a_1|\Delta\rho^*|^{\delta-1}]}. \tag{3}$$

Let $|\Delta\rho^*| = x$ or $y$, $x = (\rho_c - \rho)/\rho_c$ and $y = (\rho - \rho_c)/\rho_c$.

From equation (3) we get for $\rho < \rho_c$

$$bt^\gamma \ln(1-x) = \frac{x^{3+\theta}}{3+\theta} - \frac{x^{2+\theta}}{2+\theta} - \frac{x^{1+\theta}}{1+\theta} + \int \frac{x^\theta}{1-x}\,dx = a(z - z_0)$$

assuming $\theta = 1/3$, i.e. $\delta = 4\frac{1}{3}$,

$$a(z-z_0) = bt^\gamma \ln(1-x) - \frac{x^{10/3}}{10/3} - \frac{x^{7/3}}{7/3} - \frac{x^{4/3}}{4/3} - \psi(x^{1/3})$$

with
$$\psi(\xi) = 3\left[\frac{1}{3}\ln\frac{(1+\xi+\xi^2)^{1/2}}{1-\xi} + \frac{1}{\sqrt{3}}\tan^{-1}\frac{\xi\sqrt{3}}{2+\xi} - \xi\right] \tag{4}$$

$$\text{for } \rho > \rho_c \; a(z-z_0) = bt^\gamma \ln(1+y) + \frac{y^{10/3}}{10/3} - \frac{y^{7/3}}{7/3} + \frac{y^{4/3}}{4/3} - f(y^{1/3})$$

where
$$f(\zeta) = 3\left[\zeta - \frac{1}{3}\ln\frac{1+\zeta}{(1-\zeta+\zeta^2)^{1/2}} + \frac{1}{\sqrt{3}}\tan^{-1}\frac{\zeta\sqrt{3}}{2-\zeta}\right]. \tag{5}$$

Equations (4) and (5) are for the case when $T \geqslant T_c$. For $T \leqslant T_c$, the density profile is obtained as follows. Below $T_c$ at a point $Q$, where the meniscus is formed (figure 1).

$$(Q) = A\left|(T-T_c)/T_c\right|^\beta = X$$

$$(Q) = A\left|(T-T_c)/T_c\right|^\beta = Y$$

$$bt^\gamma \ln(1-X) + \frac{X^{19/3}}{19/3} + \frac{X^{16/3}}{16/3} + \frac{X^{13/3}}{13/3} = a(z_1 - Q) = \tilde{\alpha}_1 \tag{6}$$

and

$$bt^\gamma \ln(1+Y) + \frac{Y^{19/3}}{19/3} - \frac{Y^{16/3}}{16/3} + \frac{Y^{13/3}}{13/3} = a(Q - z_2) = \tilde{\alpha}_2. \tag{7}$$

Here $a = g\rho_c K_T^0/a_1$ and $b = 1/a_1$, $X$, $Y$, $\tilde{\alpha}_1$, $\tilde{\alpha}_2$ can be calculated from the coexistence curve data.

Equations (6) and (7) form the boundary conditions for determining $z_1$ and $z_2$.

If $\Delta\bar{\rho} = 0, Q = h/2$, where $\bar{\rho}$ is the average concentration and $h$ is the height of the cell

$$z_1 = (h/2) + (\tilde{\alpha}_1/a),$$

$$z_2 = (h/2) - (\tilde{\alpha}_2/a).$$

Therefore we get the density profile by solving,

for $\rho < \rho_c$

$$bt^\gamma \ln(1-x) + \frac{x^{19/3}(z)}{19/3} + \frac{x^{16/3}(z)}{16/3} + \frac{x^{13/3}(z)}{13/3} = a\left(\frac{h}{2} + \frac{\tilde{\alpha}_1}{a} - z\right) \tag{8}$$

for $\rho > \rho_c$

$$bt^\gamma \ln(1+y) + \frac{y^{19/3}(z)}{19/3} - \frac{y^{16/3}(z)}{16/3} + \frac{y^{13/3}(z)}{13/3} = a\left(z - \frac{h}{2} + \frac{\tilde{\alpha}_2}{a}\right). \tag{9}$$

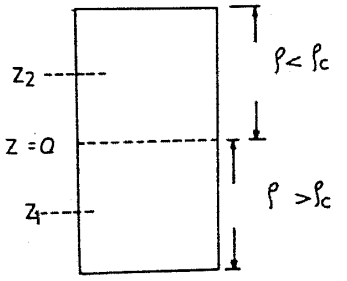


**Figure 1.** Relative positions of the meniscus for $T = T_c$.

Equations (8) and (9) give the density profile below $T_c$.

2.2 *Velocity of sound*

The isothermal velocity of sound is given by

$$C^2(z) = (\text{Bulk modulus/Density}) = (1/K_T\bar{\rho}).$$

From the equation of $K_T$, we get

$$1/C^2(z) = \frac{\rho K_T^0}{[t^\gamma + a_1 |\Delta\rho^*|^{\delta-1}]}. \tag{10}$$

If one also considers the stratification of density due to gravity (Chatterjee and Gopal 1983) one finds that the velocity of sound also depends on $d\rho/dz$ and $d^2\rho/dz^2$. Including the density stratification, one gets the velocity of sound as

$$\frac{1}{C_{\text{eff}}^2} = \frac{1}{C^2} + \frac{1}{\omega^2}\left[\frac{1}{2\rho}\frac{\partial^2\rho}{\partial z^2} - \frac{3}{4}\left(\frac{1}{\rho}\frac{\partial\rho}{\partial z}\right)^2\right], \tag{11}$$

$\omega$ is the frequency of the sound wave. This correction term will become important at lower frequencies.

2.3 *Isothermal compressibility*

Consider the fluid column to be made up of many layers each of volume $V_n$. The total change in volume $= \sum_n \frac{\partial V_n}{\partial p}\delta P$

$$= \sum \frac{1}{v_n}\frac{\partial V_n}{\partial P} v_n \delta P = \int_0^h K_T(z)\, A\, dz\, \delta P.$$

$$\bar{K}_T = \frac{1}{V}\frac{\Delta V}{\Delta P}$$

$$= \frac{1}{h}\int_0^h K_T(z)\,dz = \frac{1}{gh}\left[\frac{1}{\rho(o)} - \frac{1}{\rho(h)}\right]$$

expressing in terms of $x$ and $y$

$$\bar{K}_T = \frac{1}{gh\rho_c}\left[\left[\frac{1}{1-x(0)} - \frac{1}{1-x(n/2)}\right] + \left[\frac{1}{1+y(n/2)} - \frac{1}{1+y(n)}\right]\right]. \tag{12}$$

If one assumes the coexistence curve to be symmetric to first order, then the compressibility exponent $\gamma$ can be found with a data which is affected by gravity by fitting it to the following equation

$$\frac{x(0)^{\delta-1}}{\delta} + bt^\gamma = \frac{ah}{2}x^{-1}(0). \tag{13}$$

The coefficients $b$ and $\gamma$ can be determined using the computer.

2.4 *Thermal expansion*

Thermal expansion shows a behaviour identical to the isothermal compressibility. It

can also be independently calculated as follows:

$$\bar{\rho}h = \text{constant} \qquad h = h_0 + \Delta h,$$

where $h_0$ is the original height of the cell and $\Delta h$ is the increase in cell height due to the increase in temperature.

$$h\frac{d\bar{\rho}}{dt} + \bar{\rho}\frac{dh}{dt} = 0, \quad \text{therefore } \frac{1}{\bar{\rho}}\frac{d\bar{\rho}}{dt} = -\frac{1}{h}\frac{dh}{dt}$$

$$\frac{dh}{dt} = \frac{dh_0}{dt} - \frac{1}{\rho_c}\frac{\partial}{\partial t}\int_0^{h_0} \rho(T, z)\,dz, \quad \text{therefore } \frac{1}{h}\frac{dh}{dt} = \frac{1}{\rho_c h}\frac{\partial}{\partial t}\int_0^{h_0} \rho(T, z)\,dz.$$

Since we have an algebraic equation for determining $\rho(T, z)$, this quantity can be evaluated.

### 2.5 *Correction to the co-existence curve*

The observed data on the coexistence curve are the average density in the cell. Considering an isotherm below $T_c$, at the point $G$ (figure 2), liquid phase has just started forming. At this point, the density at which the gas and liquid coexist is $\rho(h)$ *i.e.* density at the bottom of the cell. At the point $L$, similarly, the coexisting density is $\rho(0)$.

$$\rho_{\text{actual}} = \rho(h) \quad \text{for} \quad \bar{\rho} < \rho_c,$$

$$\rho_{\text{actual}} = \rho(0) \quad \text{for} \quad \bar{\rho} > \rho_c.$$

Therefore when the real coexisting densities are replaced for the average density, the coexistence curve becomes sharper and one can eliminate the spurious flat region at the top of the coexistence curve.

## 3. Results and discussion

In this section, the results of computation are presented. The system chosen for computation is Xe, for which extensive studies exist. The values of the parameters used are given in table 1.

The density profile has been calculated with varying parameters, the average density being taken to be equal to the critical density for all the calculations. Figure 3 gives the density profile at $T = T_c$ for different cell heights, 1 mm, 1 cm and 10 cm. All the other computations are carried out with the cell height as 1 cm. We find that the departure from the critical density at the top and bottom of the cell is nearly 9·6 % for a 1 cm cell. It

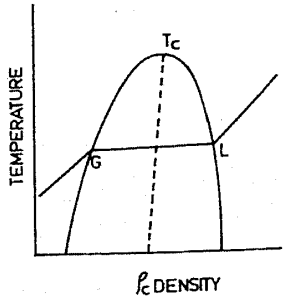


**Figure 2.** Schematic diagram of a coexistence curve for calculating corrections to gravity effect.

**Table 1.** Relevant parameters for Xe used in the computation.

| | |
|---|---|
| $T_c = 289{\cdot}734\,\mathrm{K}$ | $\gamma = 1{\cdot}19$ |
| $P_c = 5{\cdot}84 \times 10^6$ Pascals | $\delta = 4{\cdot}33$ |
| $\rho_c = 1110\,\mathrm{kg/m^3}$ | $D = 1{\cdot}5$ |
| $\beta = 0{\cdot}325$ | |

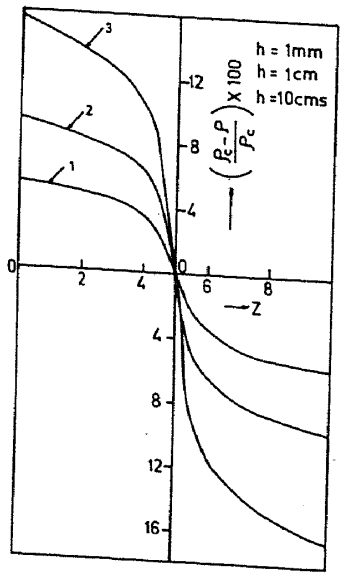


**Figure 3.** Density profile at $T = T_c$, for different cell height.

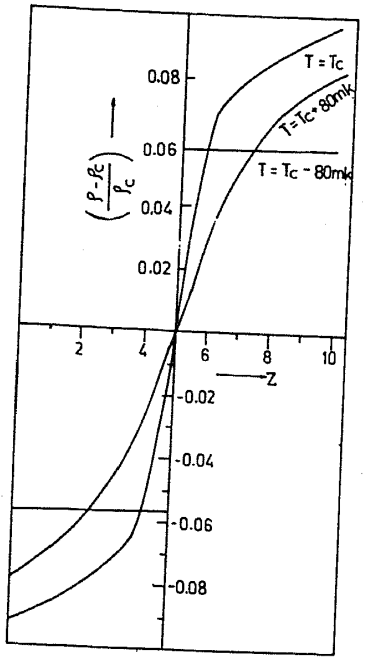


**Figure 4.** Density profile for a 1 cm cell for different temperatures.

is as much as 5·5% for a 1 mm cell and 16·6% for a 10 cm cell. Figure 4 shows the density gradient at three different temperatures $T = T_c - 80$ mK, $T = T_c$, and $T = T_c + 80$ mK. For $T_c + 80$ mK, we have a maximum density gradient of 8·3% whereas for $T_c - 80$ mK we have a discontinuity at the interface with $|(\rho - \rho_c)/\rho_c| = 0{\cdot}27$, in keeping with the coexistence curve, while the density remains almost constant on both the gaseous and liquid phases. The density gradient or profile to be expected at different gravitational fields is shown in figure 5. The maximum gradient at the top and bottom of the cell is almost 84% for $g = 10^{+5}$ but it is only 0·2% for $g = 10^{-5}$. High gravitational fields are obtained in a centrifuge and if the critical phenomena experiments are carried out in space, then very low gravitational fields are encountered.

Figure 6 shows the computation of the velocity of sound for different cell heights. The velocity of sound is normalised in the graphs. The velocity of sound goes to a minimum at the centre of the cell as $\rho(z) = \rho_c$ at that point, its value at the centre goes to zero when $T = T_c$. The velocity of sound for different $g$ values is shown in figure 7. The velocity increases by an order of magnitude for $g \sim 10^5$ in keeping with the high density

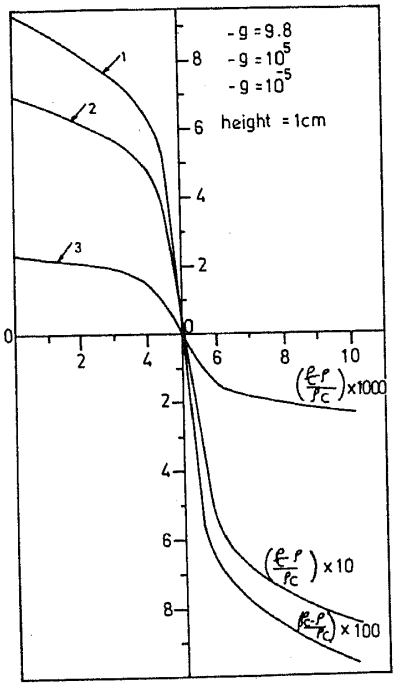


**Figure 5.** Density profile for a 1 cm cell, for different $g$ values.

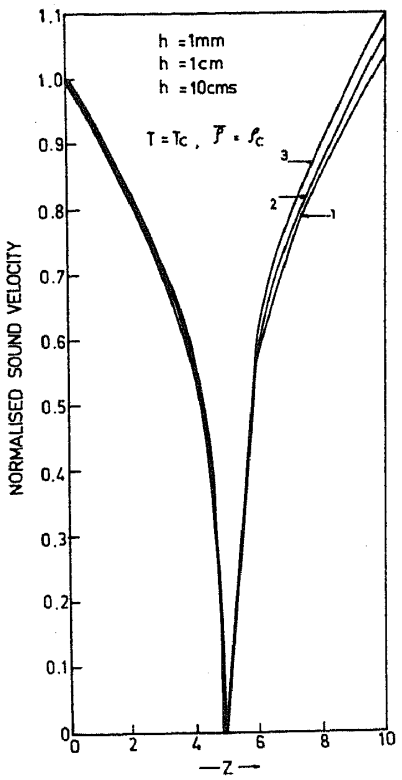


**Figure 6.** Velocity of sound at $T = T_c$ for different cell heights.

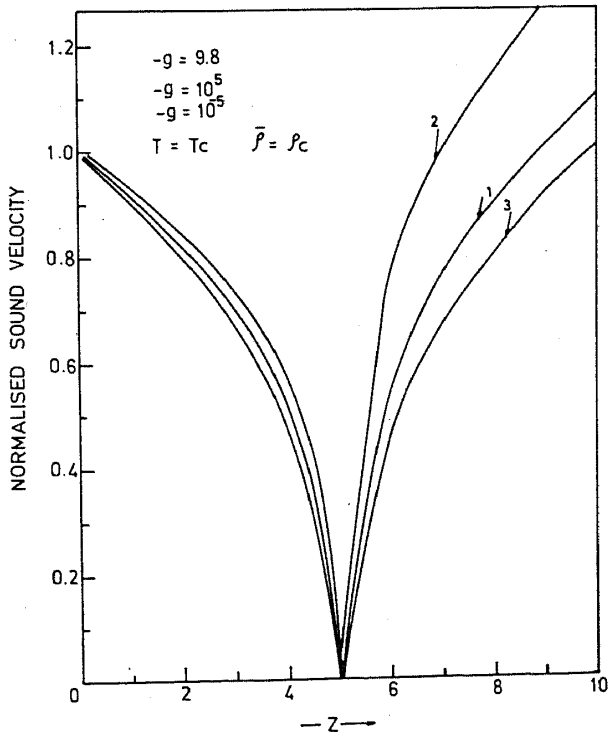


**Figure 7.** Velocity of sound at $T = T_c$ for a 1 cm cell at different $g$ values.

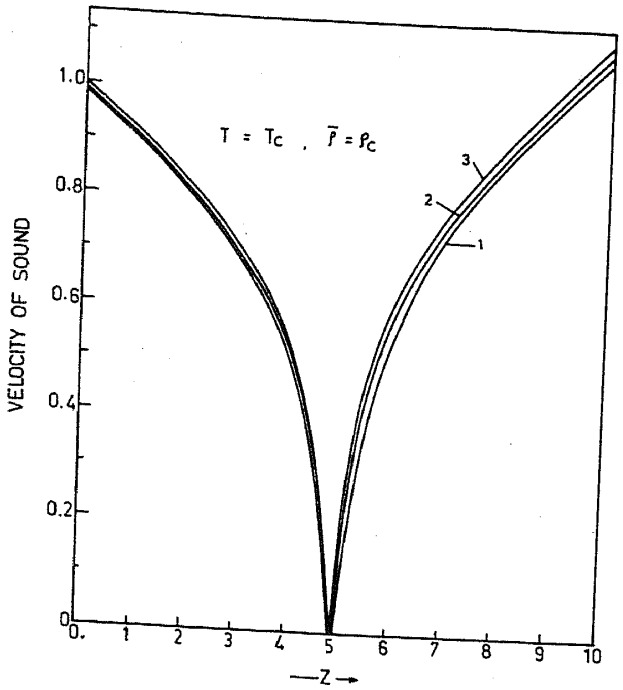


**Figure 8.** Correction to the velocity of sound at $T = T_c$ for a 1 cm cell due to the stratification of the fluid layer. 1. No correction; 2. Correction for 100 Hz; 3. Correction for 50 Hz.

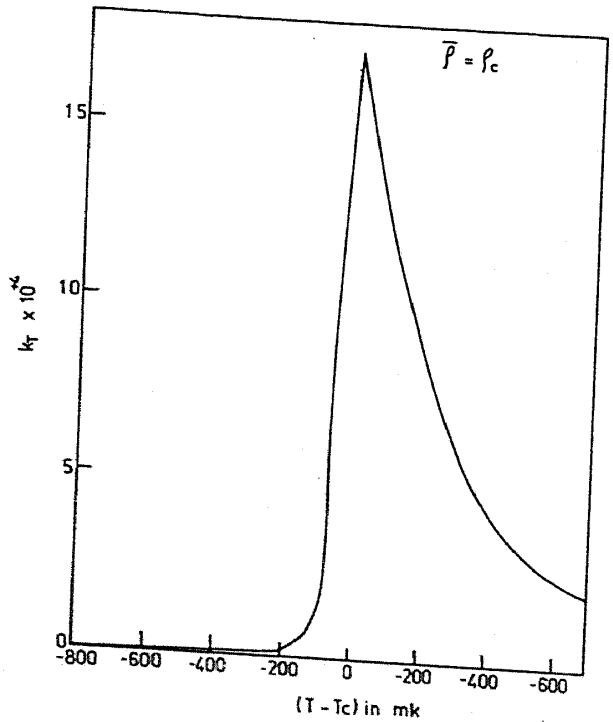


**Figure 9.** Average isothermal compressibility as a function of temperature for a 1 cm cell.

gradient but goes to zero at the centre; similarly the velocity is very low for $g \sim 10^{-5}$ but goes to zero at the centre of the cell. In figure 8, we show the correction to the sound velocity when stratification of the fluid layer is considered. The contribution of $d\rho/dz$ and $d^2\rho/dz^2$ becomes noticeable only at very low frequencies.

Figure 9 shows the behaviour of the average isothermal compressibility as a function of temperature. Since the entire cell is not at the critical density, the divergence in the compressibility gets smeared out. A simple procedure has been given in §2 on the determination of the correct exponent $\gamma$ from the experimentally observed data.

Figure 10 shows a simulated coexistence curve using the equation

$$\left|\frac{\rho-\rho_c}{\rho_c}\right| = B\left|\frac{T-T_c}{T_c}\right|^{\beta}.$$

The value of $B$ is taken as 3·51 (Estler *et al* 1975) and $\beta$ is taken as 0·325. The coexistence curve is symmetric as we have considered the coefficient $B$ to be the same for both sides of the coexistence curve. The dotted curve represents the coexistence curve that will be observed when $g = 9{\cdot}8$ . . . As the height of the experimental cell increases, the spurious flat region at the top of the coexistence curve also increases because of the increased density gradient.

We have so far outlined a simple procedure for calculating the density profile and gravity corrections to some of the thermodynamic properties. The computations involved are very simple but are found to give values which agree well with the values already reported in literature. The experimental study of the perturbations due to gravity has been largely qualitative or semiquantitative, though the first such study was

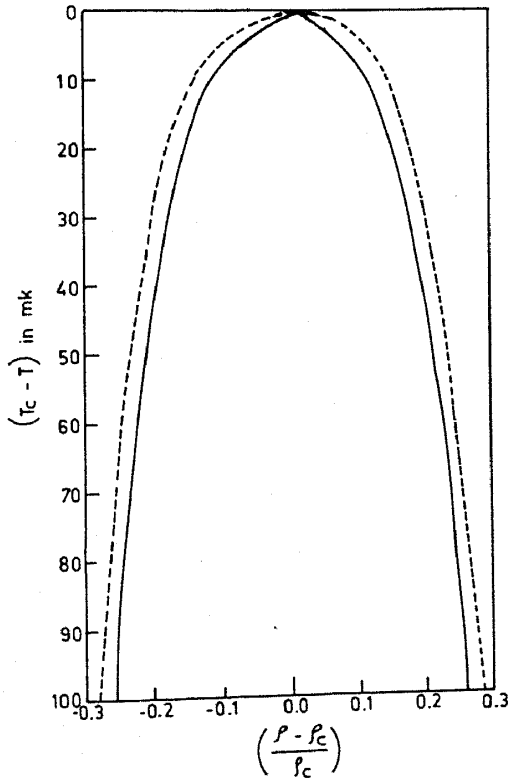


**Figure 10.** Correction to the coexistence curve for a 1 cm cell at $g = 9{\cdot}8$.

made quite some time ago (Gouy 1892). As indicated in the various papers, (Sengers and Sengers 1978; Moldover *et al* 1979; Kumar *et al* 1983), this is because of the many experimental difficulties in studying the phenomena quantitatively. In fact in most of the experiments, one really tries to eliminate or at least minimise the gravity effect by stirring the experimental cell. But the other effects of stirring are not known. The gravity corrections to specific heat and in light scattering experiments will be considered separately.

**Acknowledgement**

The authors wish to thank the CSIR, DST and the IISC-ISRO Space Technology Cell for financial help.

**References**

Chatterjee S, Vani V, Guha S and Gopal E S R 1983 *Nucl. Phys. and Solid State Phys. India* 26C (to appear)
Chatterjee S and Gopal E S R 1983 *J. Acoust. Soc. India* (to appear)
Estler W T, Hocken R, Charlton T and Wilcox L K 1975 *Phys. Rev.* A12 2118
Gouy A 1892 *C R Acad. Sci. Paris* **115** 720
Hohenberg P C and Barmatz M 1972 *Phys. Rev.* **A6** 289
Kumar A, Krishnamurthy H R and Gopal E S R 1983 *Phys. Rep.* **98** 57
Moldover M R, Sengers J V, Gammon R W and Hocken R J 1979 *Rev. Mod. Phys.* **51** 79
Sengers J V and Levelt Sengers J M H 1988 *Progress in liquid physics* (ed.) A Croxton Clive (New York: John Wiley)
Stanley H E 1971 *Introduction to phase transition and critical phenomena* (Oxford: Clarendon Press) Chap. 3

**Note added to the proof:**

In the above calculations the isothermal velocity of sound has been evaluated. This is the valid expression for sound-velocity in the high frequency range, i.e. for frequencies greater than $\omega_0 = C^2/\chi$ where $\chi$ is the thermal diffusivity and $C$, the velocity of sound in the medium. When the above condition is not satisfied, the sound velocity expression has to be replaced by the adiabatic velocity of sound. $C = (\rho K_s)^{-1/2}$; $K_s$ being the adiabatic compressibility. Our preliminary estimates show that in the critical region the isothermal velocity of sound gives a correct description for frequencies above a few hundred cycles per second. A detailed calculation of the above phenomena is now being undertaken.